Anisotropic flow measurements from RHIC to SIS

Arkadiy Taranenko[1,*]

[1]National Research Nuclear University MEPhI, Moscow, Russia

Abstract. Relativistic heavy-ion collisions provide a unique opportunity to study the expansion dynamics and the transport properties of the produced strongly interacting matter. This article reviews the recent results of anisotropic flow measurements for collision energies from $\sqrt{s_{\rm NN}}$ = 200 to 2 GeV.

1 Introduction

The heavy-ion experiments at the Relativistic Heavy Ion Collider (RHIC) and the Large Hadron Collider (LHC) have established the existence of a strongly coupled Quark Gluon Plasma (sQGP) [1, 2], a new state of nuclear matter with partonic degrees of freedom and with low specific shear viscosity η/s, i.e. the ratio of shear viscosity η to entropy density [3, 4]. Lattice QCD calculations [5] indicate that the quark-hadron transition is a smooth crossover at top RHIC energies and above (small μ_B). The possible region of a first order phase transition is expected at larger values of μ_B (lower beam energies), suggesting the existence of a critical end point (CEP) [6]. Thus, a current strategy for experimental mapping of the QCD phase diagram is centered on beam energy scans (BES), which sample reaction trajectories with the broadest possible range of μ_B and T values. The existing BES programs include: programs BES-I and BES-II of STAR experiment at RHIC for Au+Au collisions at $\sqrt{s_{\rm NN}}$ = 3-200 GeV (collider + fixed target) [7–9] and program of NA61/SHINE fixed target experiment at SPS for the different colliding systems (Be+Be, Ar+Sc Xe+La, Pb+Pb) at $\sqrt{s_{\rm NN}}$ = 5.1-17.3 GeV [10]. The future experiments at Nuclotron-based Ion Collider fAciilty (NICA) [11] and Facility for Antiproton and Ion Research (FAIR) [12] will explore the phase diagram at high baryon density region.

The anisotropic flow, as manifested by the anisotropic emission of particles in the plane transverse to the beam direction, is one of the important observable sensitive to the transport properties of the strongly interacting matter: the equation of state (EOS), the speed of sound (c_S) and the value of η/s [3, 4]. The azimuthal anisotropy of produced particles can be quantified by the Fourier coefficients v_n in the expansion of the particles azimuthal distribution as: $dN/d\phi \propto 1 + \sum_{n=1} 2v_n \cos(n(\phi - \Psi_n))$ [13–15], where n is the order of the harmonic, ϕ is the azimuthal angle of particles of a given type, and Ψ_n is the azimuthal angle of the nth-order event plane. The $n^{\rm th}$-order flow coefficients v_n can be calculated as $v_n = \langle\cos[n(\varphi - \Psi_n)]\rangle$, where the brackets denote an average over particles and events. In this work, we briefly review and discuss the recent results of the measurements of directed (v_1), elliptic (v_2) and triangular (v_3) flow for collision energies from $\sqrt{s_{\rm NN}}$ = 200 GeV (RHIC) to 2 GeV (SIS).

Elliptic (v_2) and triangular (v_3) are the dominant flow signals and have been studied very

*e-mail: AVTaranenko@mephi.ru

extensively both at top RHIC and LHC energies. Relativistic viscous hydrodynamics has been successful in describing the observed v_2 and v_3 signals for produced particles in the collisions of heavy-ion systems and the overall good agreement between data and model calculations can be reached for small values of η/s closed to the lower conjectured bound of $1/4\pi$ [3, 4, 16]. In this model framework, the values of the coefficients v_n (for $p_T < 3$ GeV/c) have been attributed to an eccentricity-driven hydrodynamic expansion of the plasma produced in the collision zone. That is, a finite eccentricity moment ε_n drives uneven pressure gradients in- and out of the event plane ψ_n, and the resulting expansion leads to the anisotropic flow of particles about this plane. The event-by-event geometric fluctuations in its initial density distribution are found to be responsible for finite elliptic flow signal v_2 in the collisions with almost zero impact parameter, and the presence of odd harmonic moments in the initial geometry ε_n and final momentum anisotropy v_n [14, 15]. The proportionality constant between v_n and ε_n is found to be sensitive to the transport properties of the matter such as as the equation of state and the specific shear viscosity η/s. The shear viscosity suppresses higher order harmonic flow coefficients $v_{n>2}$ more strongly than the elliptic flow signal v_2. The v_n data at top RHIC energy and LHC seem to follow the "acoustic scaling" for anisotropic flow, which suggests that viscous corrections to v_n/ε_n grow exponentially as n^2 and $1/(\bar{R}T)$ [17, 18, 24]:

$$\frac{v_n(p_T, \text{cent})}{\varepsilon_n(\text{cent})} \propto \exp\left[-n^2\beta'\right],\ \beta' \propto \frac{\eta}{s}\frac{1}{\bar{R}T} \propto \frac{\eta}{s}\frac{1}{(dN_{ch}/d\eta)^{1/3}}, \tag{1}$$

where T is the temperature, $\bar{R}$ is the transverse size of the collision zone. For a given harmonic number n, this equation indicates a characteristic linear dependence of $\ln(v_n/\varepsilon_n)$ on $1/(\bar{R}T)$, with a slope proportional to η/s [17, 18, 24]. The dimensionless size $\bar{R}T$ is approximately proportional to $(dN_{ch}/d\eta)^{1/3}$, where $dN_{ch}/d\eta$ is the charge particle multiplicity density [25]. The recent data from STAR collaboration indicate that v_2/ε_2 versus $(N_{ch})^{-1/3}$ has the same slope for charged hadrons from six different colliding systems: U+U, Au+Au, Cu+Au, Cu+Cu, d+Au and p+Au collisions at top RHIC energy [20], see left panel of Fig. 1. According to the "acoustic scaling" the value of this slope is proportional to η/s. The validation of the scaling relations for so many different colliding systems strongly support the hydrodynamic picture and may indicate that the value of η/s is very similar for different systems.

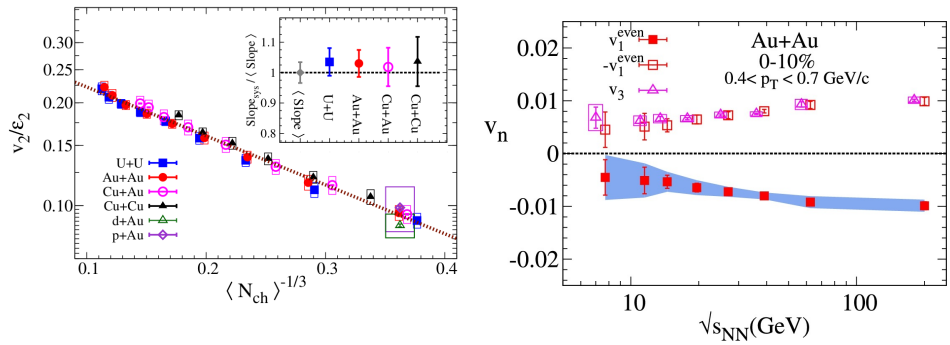

Figure 1. Left: v_2/ε_2 versus $(N_{ch})^{-1/3}$ for charged hadrons from U+U, Au+Au, Cu+Au, Cu+Cu, d+Au and p+Au collisions at top RHIC energy. The picture with STAR data was taken from [20]. The dotted line represents an exponential fit to the data with Eq.1. Right: STAR data for $\sqrt{s_{\rm NN}}$ dependence of v_1^{even} and v_3 for charged hadrons with $0.4 < p_T < 0.7$ GeV/c in 0-10% central Au+Au collisions [19]

There are two components in directed flow $v_1(y) = v_1^{odd}(y)+v_1^{even}(y)$ [19, 22]. Rapidity-odd component of directed flow v_1^{odd} is the first harmonic coefficient in the Fourier expansion of the final-state azimuthal distribution of particles relative to the reaction plane (a plane defined by the impact parameter vector and the beam direction) and describes a collective sideward motion of emitted particles $v_1^{odd}(y) = -v_1^{odd}(-y)$. In symmetric collisions, such as Au+Au, the rapidity-even component v_1^{even} ($v_1^{even}(y) = v_1^{even}(-y)$) arises from event-by-event fluctuations in the initial nuclei and it is proportional to the fluctuations-driven dipole asymmetry ε_1 of the system [21]. Similar to v_2 and v_3 the magnitude of v_1^{even} is sensitive to η/s. The excitation functions for v_1^{even} and v_3 of charged hadrons from 0-10% central Au+Au collisions are shown in the right panel of Fig. 1. The results were obtained by STAR experiment during the BES-I scan at RHIC [19]. The v_1^{even} data were reflected about zero to facilitate a comparison of the magnitudes. The comparison indicates very similar magnitudes and $\sqrt{s_{\rm NN}}$ dependence for $|v_1^{\rm even}|$ and v_3. Both signals decrease with decreasing $\sqrt{s_{\rm NN}}$. The excitation functions of v_1^{even} and v_3 are expected to provide new experimental input to ongoing theoretical efforts to discern between different initial-state models and make precision extractions of $\eta/s(T)$ [19].

2 Directed flow

The search for the predicted first-order phase transition between hadronic and QGP phases is one of the goals of the present beam energy scan programs at RHIC and SPS [7, 8]. Such a transition can also be characterized by a dramatic drop in the pressure, or a softening of the Equation of State (EOS) [32]. The signals like anisotropic flow are very promising due to their sensitivity to EOS. The rapidity-odd component of directed flow (v_1^{odd}) can probe the very early stages of the collision as it is generated during the passage time of the two colliding nuclei $t_{pass} = 2R/(\gamma_s\beta_s)$, where R is the radius of the nucleus at rest, β_s is the spectator velocity in c.m. and γ_s the corresponding Lorentz factor, respectively. Both hydrodynamic and transport model calculations indicate that the directed flow of charged particles, especially baryons at midrapidity, is very sensitive to the equation of state [31, 32]. The slope of the rapidity dependence dv_1/dy close to mid-rapidity is a convenient way to characterize the overall magnitude of the rapidity-odd component of directed flow signal [22]. A minimum in dv_1/dy in the midrapidity region ($y \sim 0$) could be related to the softening of equation-of-state due to the first order phase transition between hadronic matter and QGP [7, 8, 22, 31, 32]. The recent directed flow results from the STAR BES-I program at RHIC ($\sqrt{s_{\rm NN}} = 7.7 - 200$ GeV) seem to support this prediction, both protons and Λ hyperons dv_1/dy show a minimum around $\sqrt{s_{\rm NN}}$=10-20 GeV [28], see left panel of Fig. 2. In general, the assumption of purely hadronic physics is disfavored by the comparison of experimental dv_1/dy results and predictions from current state-of-the-art models [7, 22, 28]. However, all current models are not able to reproduce the basic trends of $\sqrt{s_{\rm NN}}$ dependence of baryon dv_1/dy-slope reported by STAR experiment. Thus, further progress in the area of model calculations of $v_1(y)$ is needed. On the experimental side, one need to perform high-statistics differential measurements of v_1 as a function of centrality, p_T, rapidity for different particle species. The statistics achieved in RHIC BES-I allow to focus the analysis dv_1/dy only on a single wide centrality bin 10-40%, see right panel of Fig. 2. The upper green curve in this panel shows the approximate upper bound of the measured dv_1/dy range for protons in central collisions (0–10%), and the lower green curve shows the approximate lower bound for peripheral collisions (60–80%). These bounds based on the preliminary STAR results [37, 42] and they indicate a remarkably strong centrality dependence. Moreover, for low energies the dv_1/dy slope for protons changes sign as a function of centrality. All these high-statistics measurements of v_1 will possible when STAR BES-II data become available.

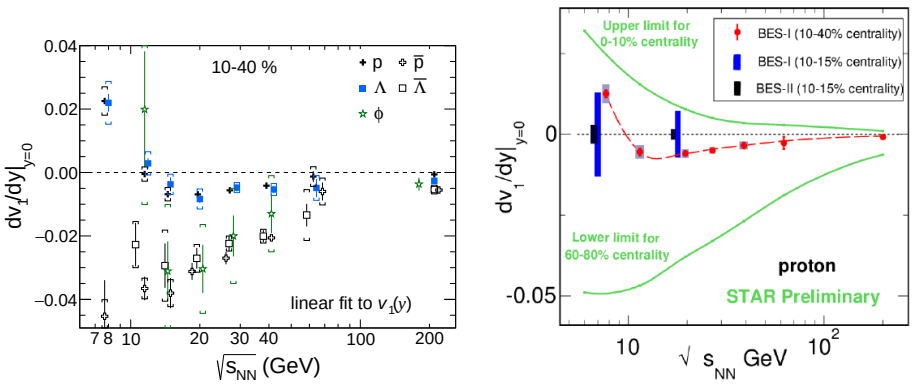

Figure 2. Left: STAR results for the beam energy dependence of the slope of rapidity-odd dv_1/dy near mid-rapidity for protons, anti-protons, Λ, $\bar{\Lambda}$ and ϕ mesons from mid-central (10-40%) Au+Au collisions. Figure is taken from [28]. Right: Expected centrality dependence for proton dv_1/dy near midrapidity for Au+Au collisions (green lines) based on STAR preliminary data from BES-I program. Figure is taken from [42]

The program of NA61/SHINE fixed target experiment at SPS(CERN) allows to perform the beam energy scan for different colliding systems (Be+Be, Ar+Sc Xe+La, Pb+Pb) in the energy range of 13-150A GeV/c ($\sqrt{s_{NN}}$ = 5.1-17.3 GeV). This also allows one to extend the flow measurements carried out by STAR RHIC beam energy scan (BES) program to a wide rapidity range, extending up to the forward region where projectile nucleon spectators appear. Fig. 3(left) shows the preliminary data of NA61/SHINE collaboration for the centrality dependence of dv_1/dy near midrapidity for protons and charged pions from Pb+Pb collisions at 30 AGeV ($\sqrt{s_{NN}}$=7.65 GeV). The data show that centrality dependence of dv_1/dy is very strong and dv_1/dy for protons is changing sign as a function of centrality. The right panel of Fig. 3 shows the p_T dependence of v_1 of protons and charged pions (π^+ and π^-) from 15-35% central Pb+Pb collisions at 30 AGeV [10].

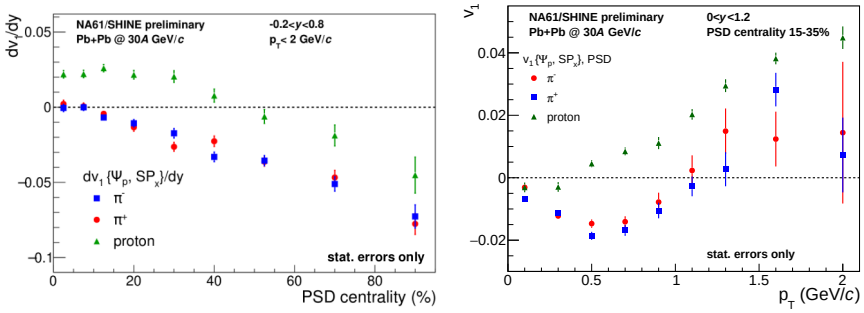

Figure 3. Left: Centrality dependence for dv_1/dy near midrapidity for protons and charged pions from Pb+Pb collisions at 30 AGeV ($\sqrt{s_{NN}}$=7.65 GeV). Right: p_T dependence of v_1 of protons and charged pions (π^+ and π^-) from 15-35% central Pb+Pb collisions at 30 AGeV ($\sqrt{s_{NN}}$=7.65 GeV). [10]

3 Elliptic flow

The elliptic flow v_2 is one of the most extensively studied observable in relativistic nucleus-nucleus collisions and was measured in different experiments in the last three decades. However, the high-statistics differential measurements of v_2 as a function of centrality, p_T, rapidity for different particle species are available only at two beam energy domains: RHIC/LHC ($\sqrt{s_{\rm NN}}$ = 30-5200 GeV) and SIS ($\sqrt{s_{\rm NN}}$ = 1 − 2 GeV). At the moment for the beam energy range from $\sqrt{s_{\rm NN}}$ = 2 to 62.4 GeV one can plot the excitation function for differential elliptic flow $v_2(p_T)$ only for protons from midcentral Au+Au collisions. This is shown in the left panel of Fig. 4, where the $v_2(p_T)$ data from three different experiments: FOPI (SIS) [23], E895 (AGS) [33] and STAR (RHIC) [36] are presented. We emphasize, however, that the available data are not derived under the same experimental conditions. The differences include: a) different methods for flow measurements, b) different rapidity coverage and c) different centrality selection: FOPI (15-29%), E895 (12-25%) and STAR (10-40%). According to the STAR BES-I data $v_2(p_T)$ for protons changes relatively little as a function of beam energy in the range $\sqrt{s_{\rm NN}}$ = 11.5 - 62.4 GeV. According to the hybrid transport + viscous hydrodynamics approach such $v_2(p_T)$ behavior may result from the interplay of the hydrodynamic and hadronic transport phase [39]. The calculations show that the hydrodynamically produced v_2 does vanish at low collision energies $\sqrt{s_{\rm NN}}$ = 5 - 7.7 GeV. However, the transport dynamics become more important at lower energies and are able to compensate for the reduction of hydrodynamically produced v_2 flow [39, 41].

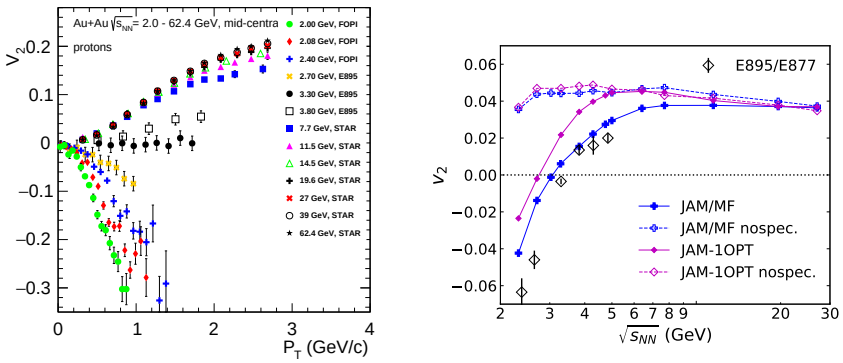

Figure 4. Left: Excitation function of differential elliptic flow $v_2(p_T)$ of protons from mid-central Au+Au collisions at energies from $\sqrt{s_{\rm NN}}$= 2 to 62.4 GeV. Data are taken from References: FOPI [23], E895 [33] and STAR [36]. Right: Excitation function of integral v_2 for nucleons in midcentral Au+Au collisions (4.6 < b < 9.4 fm) from hadronic transport model JAM [30] with first-order phase transition and mean-field simulations with (closed symbols) and without spectator interactions (open symbols). Figure is taken from [30]

At lower beam energies $\sqrt{s_{\rm NN}}$ < 11 GeV, shadowing effects by the spectator matter play an important role for the generation of elliptic flow. In the energy range $\sqrt{s_{\rm NN}}$ = 11.5 − 2 GeV, the passage time t_{pass} increases from 2 fm/c to 16 fm/c. Right panel of Fig. 4 summarizes the effect of spectator shadowing on the elliptic flow of nucleons at midrapidity as a function of beam energy. The results were obtained using the hadronic transport model JAM [30] for mean-field simulation as well as simulations with a first-order phase transition. For a broad range of beam energies ($\sqrt{s_{\rm NN}}$ = 2 − 7 GeV), the elliptic flow results can be understood in terms of a delicate balance between (i) the ability of pressure developed early in the

reaction zone, to effect a rapid transverse expansion of nuclear matter, and (ii) the passage time t_{pass} for removal of the shadowing of participant hadrons by the projectile and target spectators [29, 30, 33]. The characteristic time for the development of expansion perpendicular to the reaction plane is $\sim R/c_s$, where the speed of sound $c_s = \sqrt{\partial P/\partial \varepsilon}$, R is the nuclear radius, P is the pressure and ε is the energy density [29, 33]. If the passage time t_{pass} is long compared to the expansion time, spectator nucleons serve to block the path of participant hadrons emitted toward the reaction plane, and nuclear matter is squeezed-out perpendicular to this plane giving rise to negative elliptic flow ($v_2 < 0$). The squeeze-out contribution should then reflect the ratio $c_s/(\gamma_0\beta_0)$. This is put into evidence in left panel of Fig. 5 where the differential elliptic flow values $v_2(p_T)$ for protons from FOPI experiment, shown for beam energies of E_{lab} = 0.6, 0.8, 1.0, 1.2 and 1.49 AGeV in Fig. 4, are plotted as a function of the normalized center-of-mass (c.m.) transverse momentum (per nucleon) $p_T^0 = p_T/m_p \cdot (\gamma_0\beta_0) = t_{pass} * p_T/m_p$. The rather good scaling observed suggest that c_s does not change significantly over beam energy range 0.6 - 1.5 AGeV.

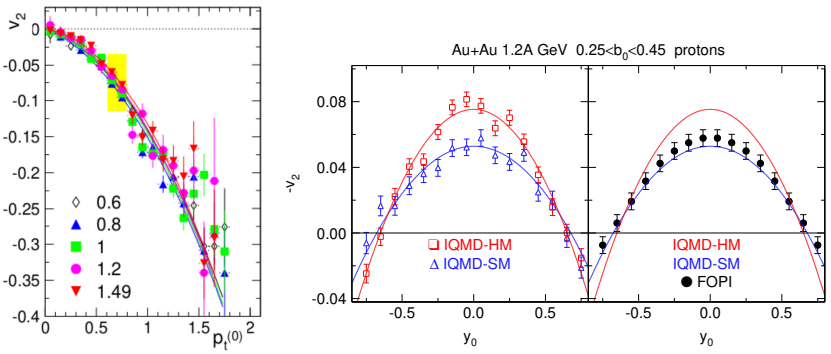

Figure 5. Left: Excitation function of differential elliptic flow $v_2(p_T^0)$ of protons from mid-central Au+Au collisions (E_{lab} = 0.6, 0.8, 1.2, 1.45 AGeV), where p_T^0 is the normalized center-of-mass (c.m.) transverse momentum (per nucleon). This is the same data points from FOPI experiment [23], plotted in the left panel of Fig. 4. The figure is taken from [23]. Right: IQMD model calculations (open symbols) for a hard (HM) and a soft (SM) EoS for elliptic flow signal -v_2 of protons as a function of the normalized rapidity y_0 for mid-central Au+Au collisions at E_{lab}=1.2 AGeV. Lines show the fit results assuming a quadratic dependence $v_2(y_0) = v_{20} + v_{22}\Delta y_0^2$. The obtained fit results (lines) in comparison with the experimental data (closed symbols) measured with the FOPI experiment (GSI) [46]. The figures are taken from [47]

The elliptic flow at SIS energies ($0.4 < E_{lab} < 1.5$ AGeV or $\sqrt{s_{\rm NN}} = 1 - 2.5$ GeV) is sensitive to the mean field and to the equation of state. Consequently, comparisons of results of high-statistics differential measurements of v_2 to model calculations can provide important constraints for the EOS. Such comparisons have been carried out for the beam energy range $0.4 < E_{lab} < 1.49$ AGeV using the data from FOPI experiment at SIS [47]. The precision in interpreting the measured high-statistics differential v_2 data has been demonstrated by the FOPI Collaboration [46, 47]. In contrast to previous work [23], they used not only protons, but also two- and three-nucleon clusters that are emitted in Au + Au collisions at $0.4 < E_{lab} < 1.49$ AGeV and that have larger flow signals than single nucleons [47]. They used not only the mid-rapidity data [23], but explored the strong dependence of v_2 on rapidity [46].

As an example the closed symbols on the right panel of Fig. 5 show the FOPI data for elliptic flow signal -v_2 of protons as a function of the normalized rapidity y_0 (rapidity normalized to the projectile rapidity in the c.m. system) for mid-central Au+Au collisions at E_{lab} = 1.2 AGeV. The data shows that elliptic flow v_2 as a function of rapidity y_0 can be well

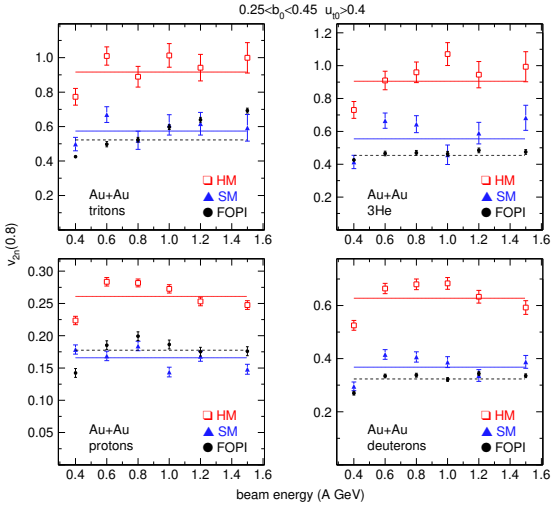

Figure 6. Elliptic flow parameter v_{2n} for protons, deuterons, tritons and ^3He as function of incident beam energy for FOPI experimental data and IQMD model calculations. The figure is taken from [47]

described by a quadratic fit $v_2 = v_{20} + v_{22} \cdot y_0^2$. The open symbols show the results of Isospin Quantum Molecular Dynamics (IQMD) model calculations for a hard (HM) and a soft (SM) EoS [47]. They introduced the new quantity v_{2n} defined by $v_{2n} = |v_{20}| + |v_{22}|$, which combines the information contained in the amplitude and the rapidity dependence of v_2. The value of v_{2n} was found to be very sensitive to the incompressibility K_0 and the in-medium nucleon-nucleon cross section [47]. Fig. 6 presents the v_{2n} value for protons, deuterons, tritons and ^3He as function of incident beam energy for FOPI experimental data and IQMD model calculations. The dependence of v_{2n} on the incident energy in the interval 0.4 to 1.5 AGeV covered by FOPI is fairly flat. This supports the previous conclusion based on the passage time scaling, that c_s does not change significantly over beam energy range 0.6 - 1.5 AGeV. The discriminating power of new variable v_{2n} between the soft and stiff parametrizations of the symmetric-matter EoS looks very convincing [47].

4 Triangular flow

Similar to directed flow [22] one may expect to observe two components in triangular flow $v_3(y) = v_3^{odd}(y) + v_3^{even}(y)$. The rapidity-even component v_3^{even} ($v_3^{even}(y) = v_3^{even}(-y)$) arises from event-by-event fluctuations in the initial nuclei and it is proportional to the fluctuations-driven ε_3 of the system. According to hybrid transport + viscous hydrodynamics model calculations [39] the rapidity-even component v_3^{even} is expected to be more sensitive to the viscous damping (than v_2) and might be an ideal observable to probe the formation of a QGP and the pressure gradients in the early plasma phase [39, 41]. The calculations show that the hydrodynamically produced v_3^{even} does vanish at low collision energies $\sqrt{s_{\rm NN}}$ = 5 - 7.7 GeV and there is no v_3^{even} signal generated by the transport dynamics in the hadronic phase [39, 41].

These conclusions [39] are supported by the STAR measurements of $v_3^2\{2\}$ for charged hadrons based on BES-I RHIC data. Fig. 7 left shows the variation of $v_3^2\{2\}$ for charged hadrons produced at mid-rapidity from 7.7 GeV up to 2.76 TeV for different bins in collision centrality [38]. At low energies $\sqrt{s_{\rm NN}} < 14.5$ GeV, the $v_3^2\{2\}$ become consistent with zero

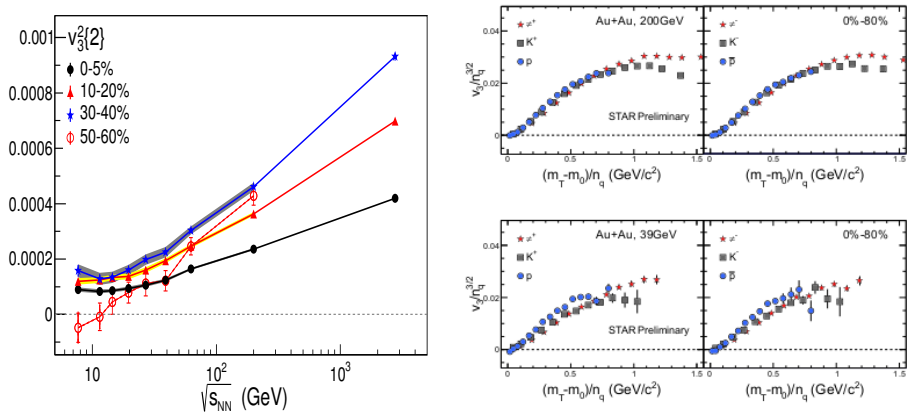

Figure 7. Left: The variation of $v_3^2\{2\}$ for charged hadrons produced at mid-rapidity from 7.7 GeV up to 2.76 TeV [34] for different bins in collision centrality. The figure is taken from [38] Right: Quark-number (n_q) scaled triangular flow, $v_3/n_q^{3/2}$ versus $(m_T - m_0)/n_q$, for charged pions, kaons and (anti)protons emerged from 0-80% central Au+Au collisions at $\sqrt{s_{\rm NN}}$ = 200 GeV (top panels) and at $\sqrt{s_{\rm NN}}$ = 39 GeV (bottom panels). The left panels represent the results for particles and right panels for anti-particles. The figure is taken from [40]

in 50-60% peripheral collisions. This result is consistent with the idea of absence of a low viscosity QGP phase in low energy peripheral collisions [39]. For more central collisions, the values of $v_3^2\{2\}$ are positive and change little from 19.6 GeV to 7.7 GeV. For the energies above 19.6 GeV, the values of $v_3^2\{2\}$ linearly increase with the $log(\sqrt{s_{\rm NN}})$ for all bins in collision centrality [38]. Fig. 7 right shows the preliminary data from STAR collaboration for v_3 of identified charged hadrons from Au+Au collisions at $\sqrt{s_{\rm NN}}$ = 200 GeV (upper panels) and 39 GeV (lower panels) [40]. The left panels represent the results for particles and right panels for anti-particles. For 200 GeV the measured v_3 values follow the $v_3/n_q^{3/2}$ versus $(m_T - m_0)/n_q$ scaling. However, for 39 GeV data one can see that the scaling is not so perfect.

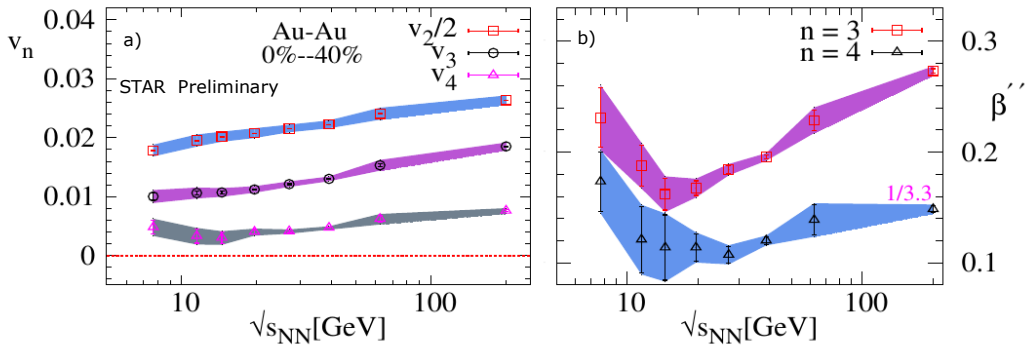

Figure 8. $\sqrt{s_{\rm NN}}$ dependence of the p_T -integrated v_n (left panel) and the estimated viscous coefficient $\beta'' \propto \eta/s$ (right panel). Results are shown for 0-40% central Au+Au collisions; the shaded lines are the systematic uncertainty. The figure is taken from [24]

The left panel of Fig. 8 shows the preliminary STAR data for the $\sqrt{s_{\rm NN}}$ dependence of the p_T integrated v_n of charged hadrons from 0-40% central Au+Au collisions [24]. It shows an essentially monotonic trend for v_2, v_3 and v_4 with $\sqrt{s_{\rm NN}}$ as might be expected for a temperature increase as $\sqrt{s_{\rm NN}}$ increases [24]. The same authors applied the "acoustic scaling" to v_n data in order to estimate the $\sqrt{s_{\rm NN}}$ dependence of η/s. Using the observation that ε_n changes very slowly with beam energy and the measurements for two different harmonics$n$ and $n^{'}$ ($n \neq n^{'}$) the Eq.1 can be simplified [24] to the viscous coefficient $\beta^{"} \propto (\eta/s) \propto (dN_{ch}/d\eta)^{1/3} ln(v_n^{1/n}/v_{n^{'}}^{1/n^{'}})$. The right panel of Fig. 8 shows the $\sqrt{s_{\rm NN}}$ dependence of the viscous parameter $\beta^{"}$ extracted from the $ln(v_3^{1/3}/v_2^{1/2})$ and $ln(v_4^{1/4}/v_2^{1/2})$ results from the left panel of Fig. 8. In contrast to v_n, the excitation function of the viscous parameter $\beta^{"}$ shows a non-monotonic behavior over the same beam energy range. A similar non-monotonic trend for η/s has been observed in the hybrid viscous hydrodynamical calculations [41], tuned to describe the STAR BES-I v_2 data.

At low beam energies available at SIS ($\sqrt{s_{\rm NN}}$=1-2.5 GeV) one clearly see the rapidity-odd component of $v_3^{odd}(y)$ ($v_3^{odd}(y) = -v_3^{odd}(-y)$). As an example Fig. 9 shows the results of HADES experiment at SIS for triangular flow (v_3) of protons in semi-central ($20-30$ %) Au+Au collisions at E_{lab}=1.23 AGeV ($\sqrt{s_{\rm NN}}$ =2.3 GeV)[45]. The right panel of Fig. 9 shows the v_3^{odd} of protons as a function of p_T in the rapidity interval $-0.45 < y_{cm} < -0.35$ together with UrQMD 3.4 model simulations with two parametrization of EoS [48]. The discriminating power of v_3^{odd} between the soft and stiff parametrizations of the symmetric-matter EoS looks very convincing [48].

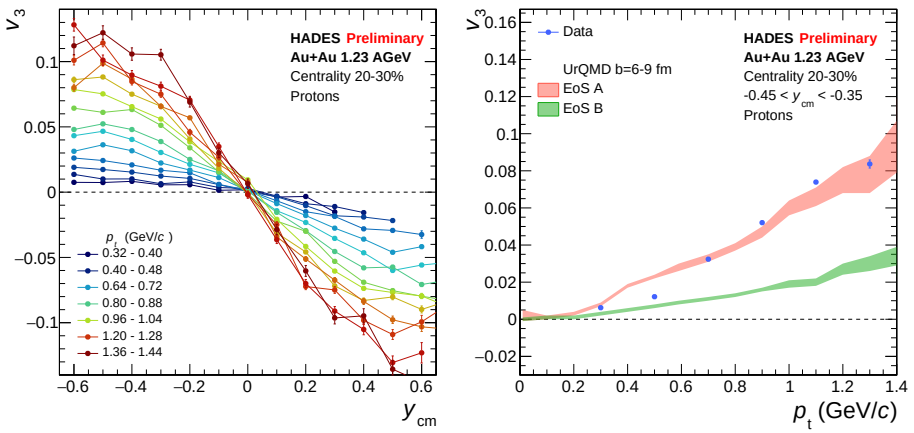

Figure 9. Left: HADES results for triangular flow (v_3^{odd}) of protons in semi-central ($20-30$ %) Au+Au collisions at 1.23 AGeV as a function of the centre-of-mass rapidity y_{cm} for different bins in transverse momentum as indicated. Right: v_3^{odd} of protons as a function of p_T in the rapidity interval $-0.45 < y_{cm} < -0.35$ together with UrQMD 3.4 model simulations with two parametrization of EoS [48]. The figures are taken from [45]

Summary

In this article, we briefly reviewed the recent results of the measurements of directed (v_1), elliptic (v_2) and triangular (v_3) flow for collision energies from $\sqrt{s_{\rm NN}}$ = 200 GeV (RHIC) to 2 GeV (SIS). The measured v_n values are found to be sensitive to transport properties of the strongly interacting matter: the equation of state (EOS), the speed of sound (c_S) and the

value of η/s. However, in order the transport properties of the strongly interacting matter as a function of the temperature T and baryon chemical potential μ_B further progress in the area of model calculations of v_n is needed. On the experimental side, one need new high-statistics differential measurements of v_n as a function of centrality, p_T, rapidity for different particle species in the high baryon density region $\sqrt{s_{\rm NN}} = 2 - 11$ GeV. The results of such measurements will be available soon from STAR experiment at RHIC (BES-II program), BM@N and MPD experiments at NICA [11] and CBM experiment at FAIR [12].

Acknowledgments. The reported study was funded by RFBR according to the research project No 18-02-00086 and the Ministry of Science and Higher Education of the Russian Federation, grant No 3.3380.2017/4.6.

References

[1] J. Adams et al. [STAR Collaboration], Nucl. Phys. A **757** (2005) 102
[2] K. Adcox et al. [PHENIX Collaboration], Nucl. Phys. A **757** (2005) 184
[3] C. Gale, S. Jeon, B. Schenke, P. Tribedy and R. Venugopalan, Phys. Rev. Lett. **110** (2013) no.1, 012302
[4] U. Heinz and R. Snellings, Ann. Rev. Nucl. Part. Sci. **63** (2013) 123
[5] Y. Aoki, G. Endrodi, Z. Fodor, S. D. Katz and K. K. Szabo, Nature **443** (2006) 675
[6] E. S. Bowman and J. I. Kapusta, Phys. Rev. C **79** (2009) 015202
[7] X. Luo, Nucl. Phys. A **956** (2016) 75
[8] D. Keane, J. Phys. Conf. Ser. **878** (2017) no.1, 012015.
[9] H. Caines, Nucl. Phys. A **967** (2017) 121.
[10] V. Klochkov et al. [NA61/SHINE Collaboration], Nucl. Phys. A **982** (2019) 439
[11] V. D. Kekelidze, Phys. Part. Nucl. **49** (2018) no.4, 457.
[12] T. Ablyazimov et al. [CBM Collaboration], Eur. Phys. J. A **53** (2017) no.3, 60
[13] S. Voloshin and Y. Zhang, Z. Phys. C **70** (1996) 665
[14] S. A. Voloshin, A. M. Poskanzer and R. Snellings, arXiv:0809.2949 [nucl-ex].
[15] R. Snellings, J. Phys. G **41** (2014) no.12, 124007
[16] R. Derradi de Souza, T. Koide and T. Kodama, Prog. Part. Nucl. Phys. **86** (2016) 35
[17] R. A. Lacey, A. Taranenko, J. Jia, D. Reynolds, N. N. Ajitanand, J. M. Alexander, Y. Gu and A. Mwai, Phys. Rev. Lett. **112** (2014) no.8, 082302
[18] R. A. Lacey, D. Reynolds, A. Taranenko, N. N. Ajitanand, J. M. Alexander, F. H. Liu, Y. Gu and A. Mwai, J. Phys. G **43** (2016) no.10, 10LT01
[19] J. Adam et al. [STAR Collaboration], Phys. Lett. B **784** (2018) 26
[20] J. Adam et al. [STAR Collaboration], arXiv:1901.08155 [nucl-ex].
[21] D. Teaney and L. Yan, Phys. Rev. C **83** (2011) 064904
[22] S. Singha, P. Shanmuganathan and D. Keane, Adv. High Energy Phys. **2016** (2016) 2836989
[23] A. Andronic et al. [FOPI Collaboration], Phys. Lett. B **612** (2005) 173
[24] N. Magdy [STAR Collaboration], J. Phys. Conf. Ser. **779** (2017) no.1, 012060.
[25] R. A. Lacey, P. Liu, N. Magdy, M. Csanád, B. Schweid, N. N. Ajitanand, J. Alexander and R. Pak, Universe **4**, no. 1, 22 (2018)
[26] R. A. Lacey and A. Taranenko, PoS CFRNC **2006** (2006) 021
[27] A. Adare et al. [PHENIX Collaboration], Phys. Rev. C **93** (2016) no.5, 051902
[28] L. Adamczyk et al. [STAR Collaboration], Phys. Rev. Lett. **120** (2018) no.6, 062301
[29] R. A. Lacey, Nucl. Phys. A **774** (2006) 199

[30] C. Zhang, J. Chen, X. Luo, F. Liu and Y. Nara, Phys. Rev. C **97** (2018) no.6, 064913
[31] D. H. Rischke, Nucl. Phys. A **610** (1996) 88C
[32] H. Stoecker, Nucl. Phys. A **750** (2005) 121
[33] C. Pinkenburg et al. [E895 Collaboration], Phys. Rev. Lett. **83** (1999) 1295
[34] L. Adamczyk et al. [STAR Collaboration], Phys. Rev. C **86** (2012) 054908
[35] L. Adamczyk et al. [STAR Collaboration], Phys. Rev. C **88** (2013) 014902
[36] L. Adamczyk et al. [STAR Collaboration], Phys. Rev. C **93** (2016) no.1, 014907 doi:10.1103/PhysRevC.93.014907
[37] P. Shanmuganathan [STAR Collaboration], Nucl. Phys. A **956**, 260 (2016)
[38] L. Adamczyk et al. [STAR Collaboration], Phys. Rev. Lett. **116** (2016) no.11, 112302
[39] J. Auvinen and H. Petersen, Phys. Rev. C **88** (2013) no.6, 064908
[40] X. Sun [STAR Collaboration], J. Phys. Conf. Ser. **535** (2014) 012005.
[41] I. A. Karpenko, P. Huovinen, H. Petersen and M. Bleicher, Phys. Rev. C **91** (2015) no.6, 064901
[42] STAR Note 598. https://drupal.star.bnl.gov/STAR/starnotes/public/sn0598
[43] C. Yang [STAR Collaboration], Nucl. Phys. A **967** (2017) 800.
[44] K. Meehan [STAR Collaboration], Nucl. Phys. A **967** (2017) 808
[45] B. Kardan [HADES Collaboration], Nucl. Phys. A **982** (2019) 431
[46] W. Reisdorf et al. [FOPI Collaboration], Nucl. Phys. A **876**, 1 (2012)
[47] A. Le Fèvre, Y. Leifels, W. Reisdorf, J. Aichelin and C. Hartnack, Nucl. Phys. A **945** (2016) 112
[48] P. Hillmann, J. Steinheimer and M. Bleicher, J. Phys. G **45** (2018) no.8, 085101